Here I bring the so far available results of our simulation to reconstruct/match the profile ^{3}He spike related to the initial Veritas particles. Recall I use the "sliding-knee model", i.e. the production function $P(D,t)$ of the source population of particles is assumed to be a broken power-law with the knee that swiftly moves in the very initial phase of evolution. In particular I consider dust particles with sizes D in between $D_1 = 10\ \mu$m and $D_2 = 1$ cm created at the source location (Veritas) so that their cumulative distribution ($P(D,t)$) is a power-law with index α_2 in the interval (D_0, D_2) and another index α_1 in the interval (D_1, D_0). Time dependence of $P(D,t)$ is entirely fold into dynamics of $D_0(t)$ for which I use

$$\log_{10}\left(\frac{D_0}{D_1}\right) = \log_{10}\left(\frac{D_2}{D_1}\right)\left[1 - \exp\left(-t/\tau_{\rm dec}\right)\right] \ . \tag{1}$$

The "sliding-knee idea" is to mimic Bill's collisional-code simulation of Veritas' SFD initial phase at small sizes. Though, obviously, the parametrization here is somewhat a toy model.

Once the particles are released from the source they migrate toward the inner solar system by the PR drag. As you remember, my simulation accounts for the semimajor effect only, disregarding any eccentricity dependence; I use 1.7 g/cm^3 as the "effective bulk density" of the TPs. On their way to the Earth, the particles got disrupted by the background projectiles with a characteristic collisional lifetime $\tau_{\rm coll}(D)$ as given by the Grün et al. (1985) lunar model. Note it takes like ~ 40 ky to migrate from Veritas to 1 AU for the 10 μm TPs. According to the Grün et al.'s model, though, the collisional lifetime of these particles at 1 AU is between $10-20$ ky, somewhat increasing for larger heliocentric distances. Thus, even the population of the very initial small Veritas particles got collisionally decimated to some extend before reaching the Earth, and obviously the whole $0.75-1$ My ^{3}He signal follows from a collisional cascade products created at the source and in the intermediate heliocentric distances. This is to keep in mind when comparing population decay at the source –Fig. 1– and the related dominance of the ^{3}He signal over the background. David N. was initially asking why the orders-of-magnitude drop at the source maps to only a factor $3-10$ over the background for ^{3}He. Part of the answer might be what I have just said, i.e. the initial small Veritas particles got to a large extend collisionally decimated. At least, this is what the model suggests.

Our toy model has a couple of free parameters whose variation will, hopefully, enable us to match the ^{3}He profile. With that I mainly mean the nice sharp onset and a quasi-exponential decrease we see on Fig. 2 (site 757) of Ken. The quantitative information is that the peak value should drop to $\sim 1/3$ up to $\sim 1/6$ within $\sim 750-800$ ky (Fig. 2, site 757). The drop depends on what we think about the singular dot in Fig. 1 of Ken. Comments?

So back to our principal free parameters: we have slopes α_1 and α_2 of $P(D,t)$ and the decay-time $\tau_{\rm dec}$ in Eq. (1); obviously the assumed collisional lifetime function –that I fix for this moment to be the Grün et al. lunar function– is another free information. I use $\alpha_1 = -2$, $\alpha_1 = -2.25$ and $\alpha_1 = -2.5$. Note that this about brackets the slope of the background dust-particle population to which the Veritas source should collisionally relax. In order to dominate the background population, α_2 should have been quite steeper. I test values in between -3 and -4. Finally, $\tau_{\rm dec}$ is set either 0.5 My or 1 My, perhaps in the ball-park of values guessed from Bill's simulation.

Each of the Figs. 2 to 5 corresponds to a particular combination of α_1 and $\tau_{\rm dec}$ values and shows the flux of Veritas particles through 1 AU for different α_2 values (these are the different panels in these figures); the flux is in arbitrary units. Moreover, different curves in each of the panels correspond to TPs in different size ranges. The uppermost red curve is for $(10-15)\ \mu$m particles, green curve is for $(15-20)\ \mu$m, blue curve is for $(20-30)\ \mu$m, and so on.

Figures 6 and 7 show the same results for $\tau_{\rm dec} = 0.5$ My and $\tau_{\rm dec} = 1$ My, respectively. As columns change we have cases of $\alpha_1 = -2, -2.25$ and -2.5, while as rows change we have cases of $\alpha_2 = -3, -3.2, -3.25, -3.3, -3.5$ and -4. So for a fixed $\tau_{\rm dec}$ we see here results for the whole tested matrix of α_1 and α_2 values.

Apparently, there is a large variation of results across the α_2 range of values -3 to -4 with the extreme values providing incompatible results (either too smeared or too sharp peak). Also the results for $\tau_{\rm dec} = 0.5$ My do usually provide too narrow peak in time, and $\tau_{\rm dec} = 1$ My seems to suit better. We note that when α_2 is "too shallow" the result is sensitive to fluke break-ups of large particles in our simulation – see e.g. the case of $\tau_{\rm dec} = 1$ My, $\alpha_1 = -2.5$ and $\alpha_2 = -3.25$. In this case a big ($\simeq 8$ mm; see the cyan curve on the corresponding panel of Fig. 16) broke early after the family was created and flooded our results with a lot of dauthter products. Obviously, the simulation runs forward and eventually such statistical effects will be suppressed, because occurence of this $\simeq 8$ mm is anomalous wrt to processed number of smaller particles, but this needs to run a lot of TPs.

So far the figures showed the particle flux at a heliocentric distance 1 AU. This signal contains the fullest possible information about what is going on with the Veritas TPs on their way toward the Earth, both as far as orbital and collisional dynamics is concerned. Obviously, to relate this information to the measured ^{3}He marine signal one needs further considerations, such as the amount of the carried ^{3}He by TPs of different sizes, its retention upon heating in the atmosphere, and also accretion probability of different-size TPs from dynamical point-of-view. A grossly simplified approach would be to assume that the amount of ^{3}He carried by particles while in the interplanetary region scales as $\propto D^2$ (cross-section) and the accretion probability scales as $\propto D$ (in response to faster PR drift of smaller particles). Overall, this would largely favourize larger TPs. However, these tend to heat enough in the atmosphere to loose their ^{3}He (e.g. Farley et al., 1997) producing a sharp cutoff in efficiency to carry this isotope for $D \geq (20 - 30)$ μm particles. At the first approximation, we might be thus satisfied with the red-curve profiles in our figures, corresponding to the smallest-bin TPs.

For sake of comparison, I have also scaled the TP flux at 1 AU by the particle cross-section and plotted the results in Figs. 9 to 12. It looks like the overall profile of the signal is robust.

Results and implications.

Finally, we show in Fig. 14 a comparison of one model with ^{3}He data reported at Sites 757 and 926. This is somewhat personally chosen run and for the final version of the paper we may agree on another one.

An implication of our model, that we've discussed in Boulder, is that there was a significant amount of dust in the size range $\sim (10 - 5000)$ μm released during the Veritas-family forming event. Fig. 1 shows how this population decays in time and Fig. 13 shows how its mass decays in time. The blue curves ($\alpha_2 = -3.5$) indicate a $50 - 100$ drop in dust mass after a couple of My.

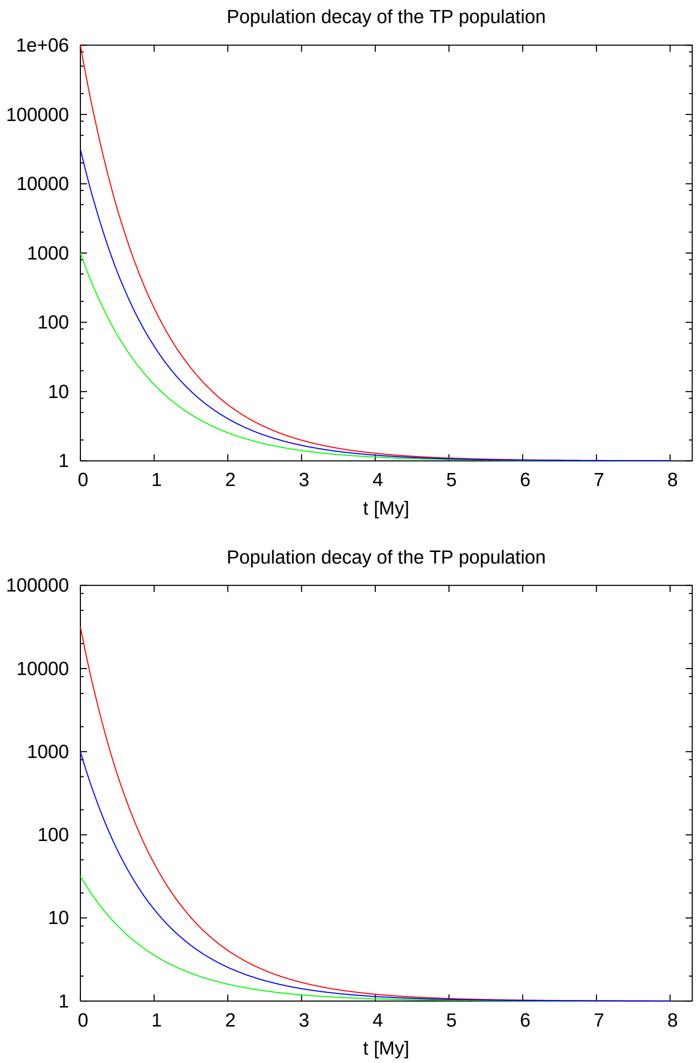

Figure 1: Models with a 'sliding knee'. Population decay – in terms of cummulative number of particles in between (D_1, D_2) – as a function of time: (i) $\alpha_1 = -2$ (top) and (ii) $\alpha_1 = -2.5$ (bottom). The three curves are for $\alpha_2 = -4, -3.5$ and -3 from top to bottom. Here we fixed $\tau_{\rm dec} = 1$ My.

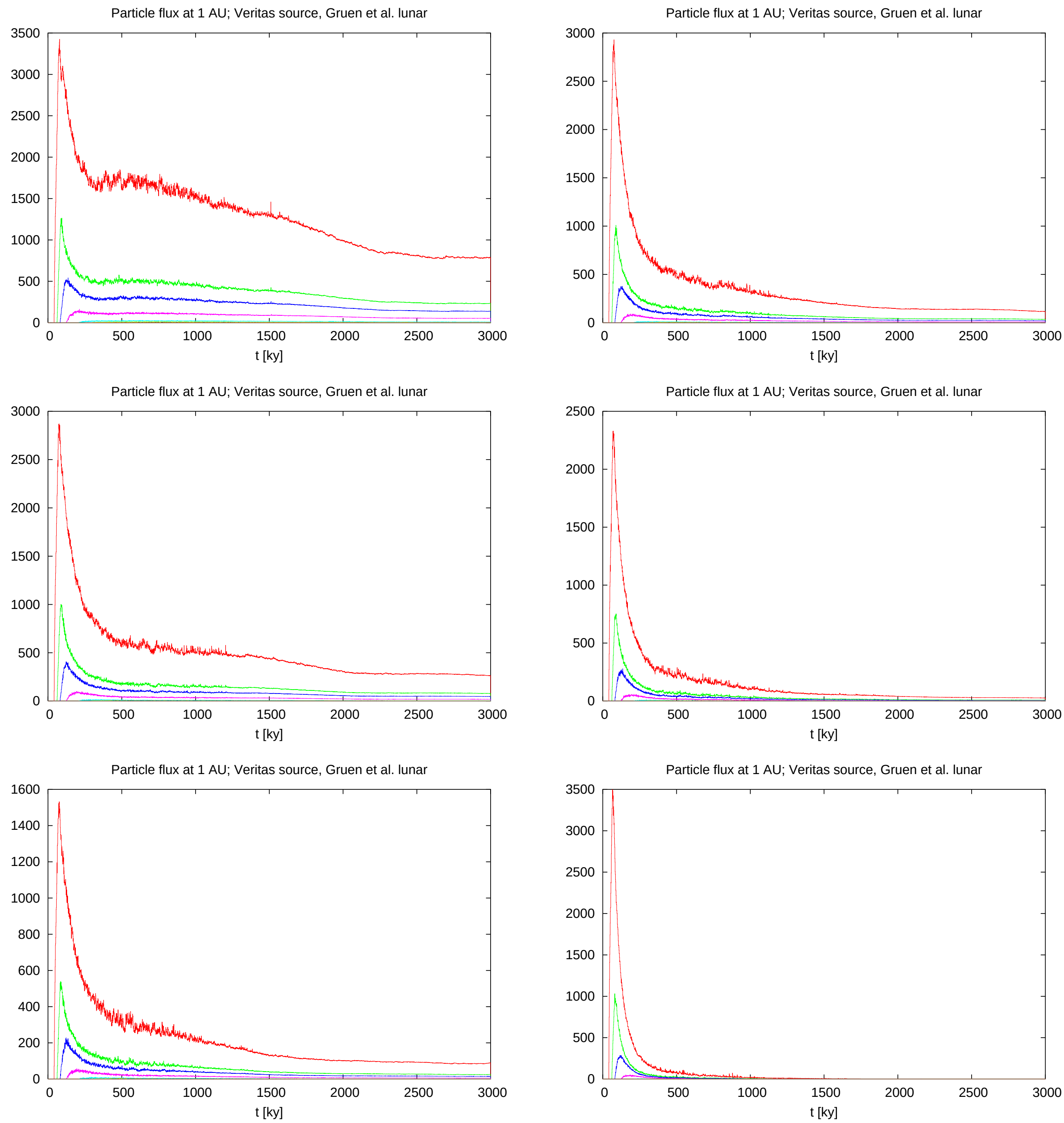

Figure 2: Models with a 'sliding knee': flux of the Veritas TPs through 1 AU heliocentric sphere as a function of time after the parent-body breakup. Here $\alpha_1 = -2$ and $\tau_{\rm dec} = 0.5$ My fixed and different panels show results for different values of α_2: (i) -3 (left, top), (ii) -3.2 (left, middle), (iii) -3.25 (left, bottom), (iv) -3.3 (right, top), (v) -3.5 (right, middle), and (v) -4 (right, bottom). Different curves in each of the panels correspond to TPs in different size ranges. The uppermost red curve is for $(10-15)$ μm particles, green curve is for $(15-20)$ μm, blue curve is for $(20-30)$ μm, and so on.

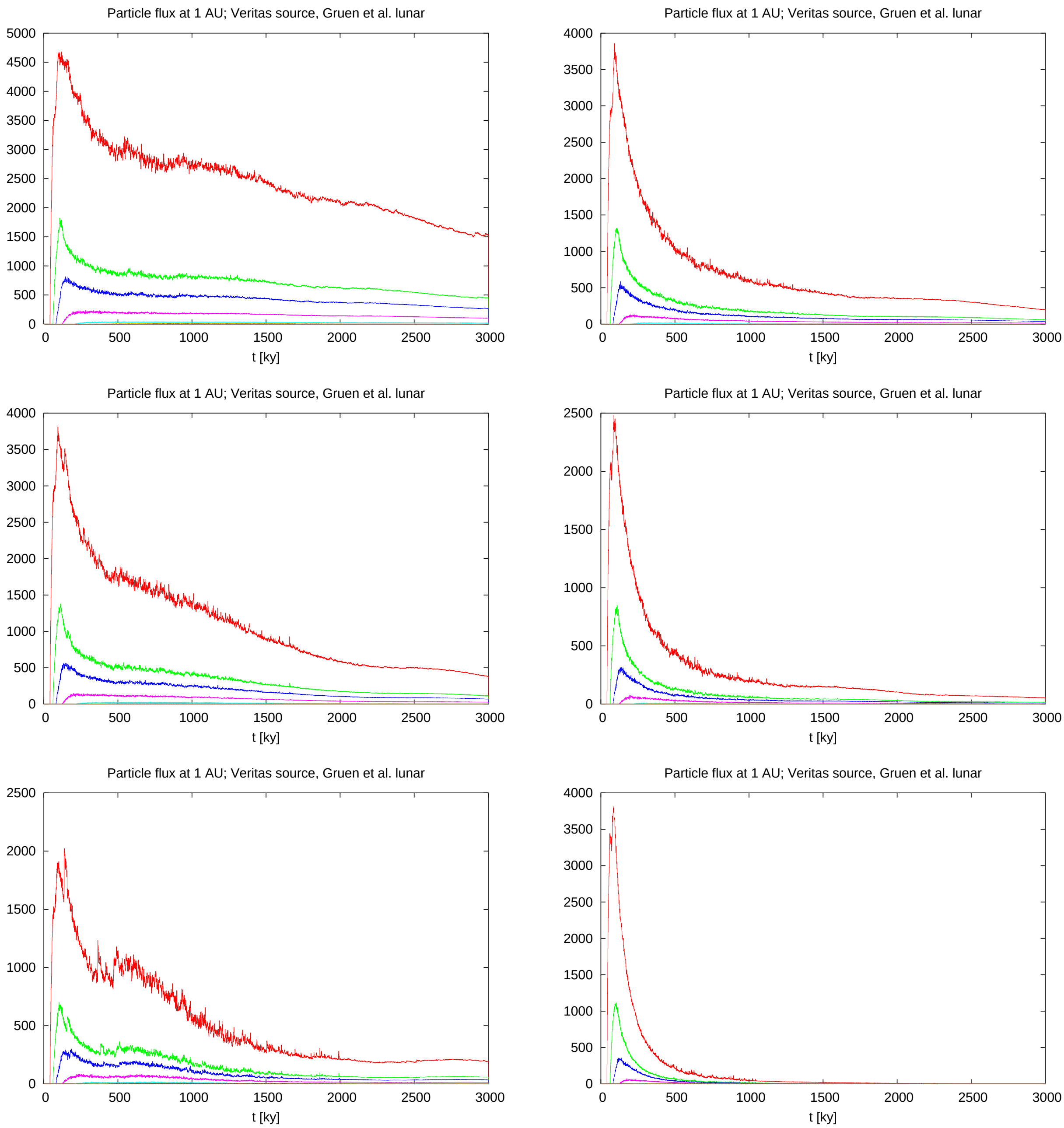

Figure 3: Models with a 'sliding knee': flux of the Veritas TPs through 1 AU heliocentric sphere as a function of time after the parent-body breakup. Here $\alpha_1 = -2$ and $\tau_{\rm dec} = 1$ My fixed and different panels show results for different values of α_2: (i) -3 (left, top), (ii) -3.2 (left, middle), (iii) -3.25 (left, bottom), (iv) -3.3 (right, top), (v) -3.5 (right, middle), and (v) -4 (right, bottom). Different curves in each of the panels correspond to TPs in different size ranges. The uppermost red curve is for $(10-15)$ μm particles, green curve is for $(15-20)$ μm, blue curve is for $(20-30)$ μm, and so on.

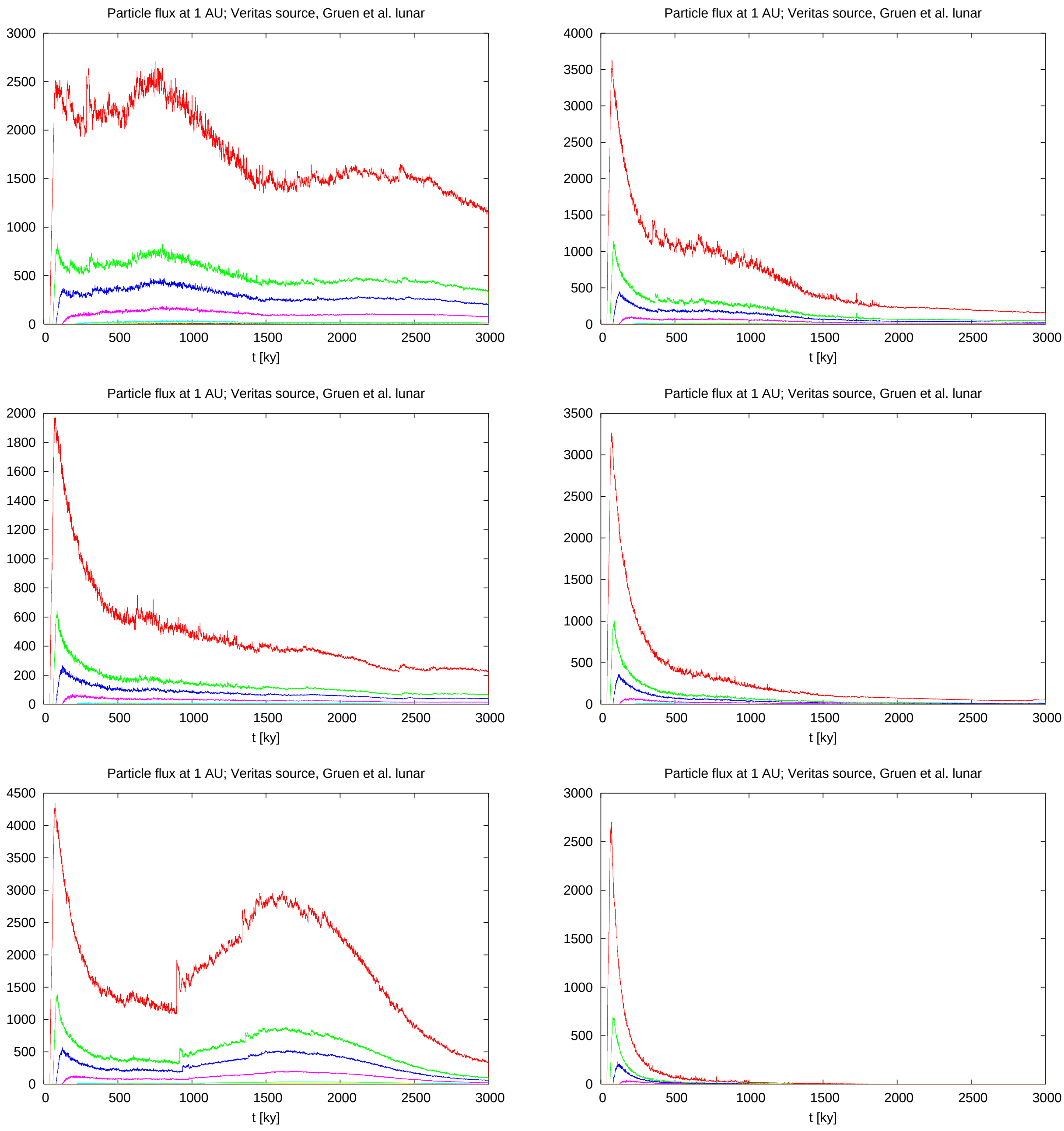

Figure 4: Models with a 'sliding knee': flux of the Veritas TPs through 1 AU heliocentric sphere as a function of time after the parent-body breakup. Here $\alpha_1 = -2.5$ and $\tau_{\rm dec} = 0.5$ My fixed and different panels show results for different values of α_2: (i) -3 (left, top), (ii) -3.2 (left, middle), (iii) -3.25 (left, bottom), (iv) -3.3 (right, top), (v) -3.5 (right, middle), and (v) -4 (right, bottom). Different curves in each of the panels correspond to TPs in different size ranges. The uppermost red curve is for $(10-15)$ μm particles, green curve is for $(15-20)$ μm, blue curve is for $(20-30)$ μm, and so on.

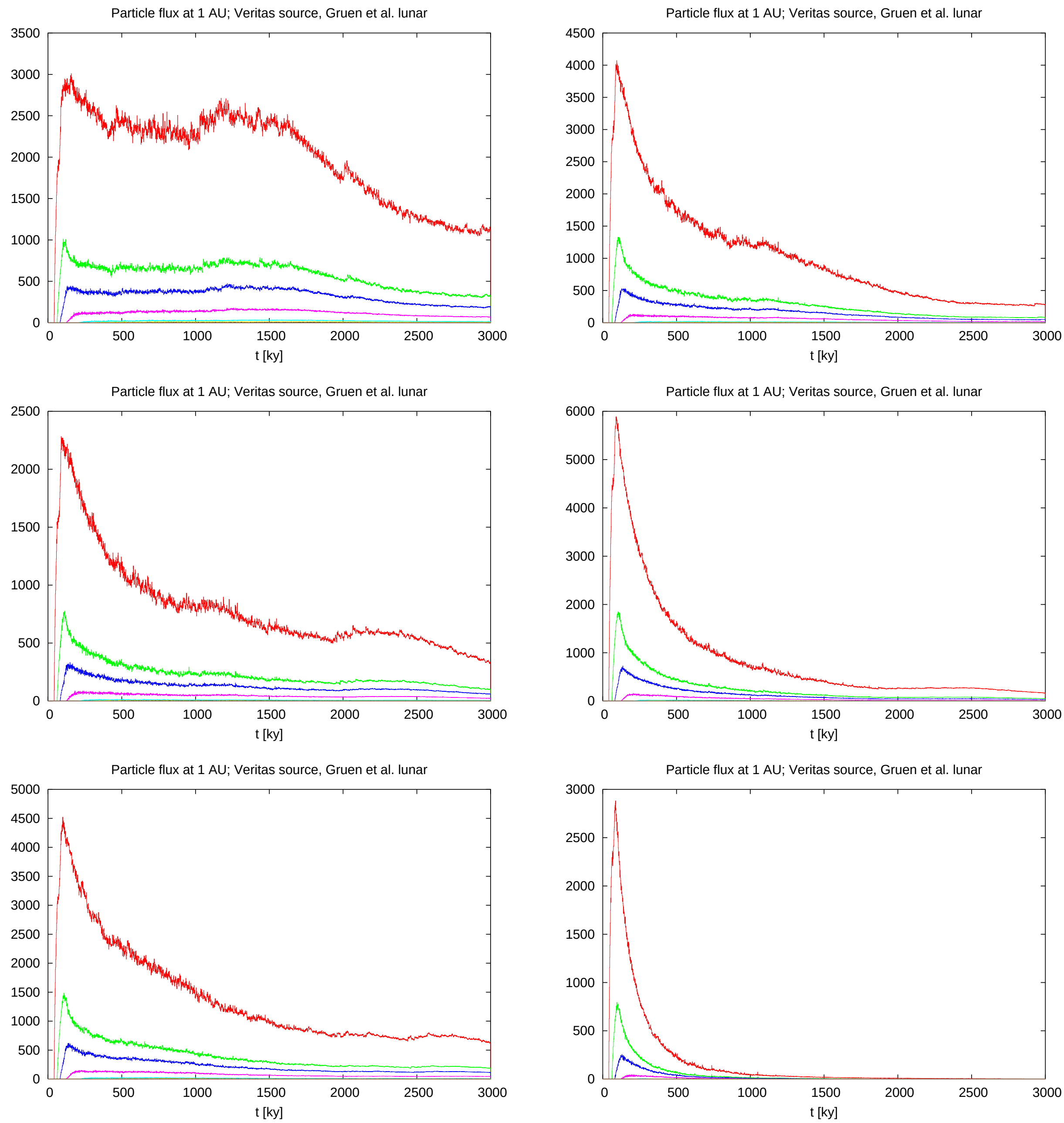

Figure 5: Models with a 'sliding knee': flux of the Veritas TPs through 1 AU heliocentric sphere as a function of time after the parent-body breakup. Here $\alpha_1 = -2.5$ and $\tau_{\rm dec} =$ 1 My fixed and different panels show results for different values of α_2: (i) -3 (left, top), (ii) -3.2 (left, middle), (iii) -3.25 (left, bottom), (iv) -3.3 (right, top), (v) -3.5 (right, middle), and (v) -4 (right, bottom). Different curves in each of the panels correspond to TPs in different size ranges. The uppermost red curve is for $(10-15)$ μm particles, green curve is for $(15-20)$ μm, blue curve is for $(20-30)$ μm, and so on.

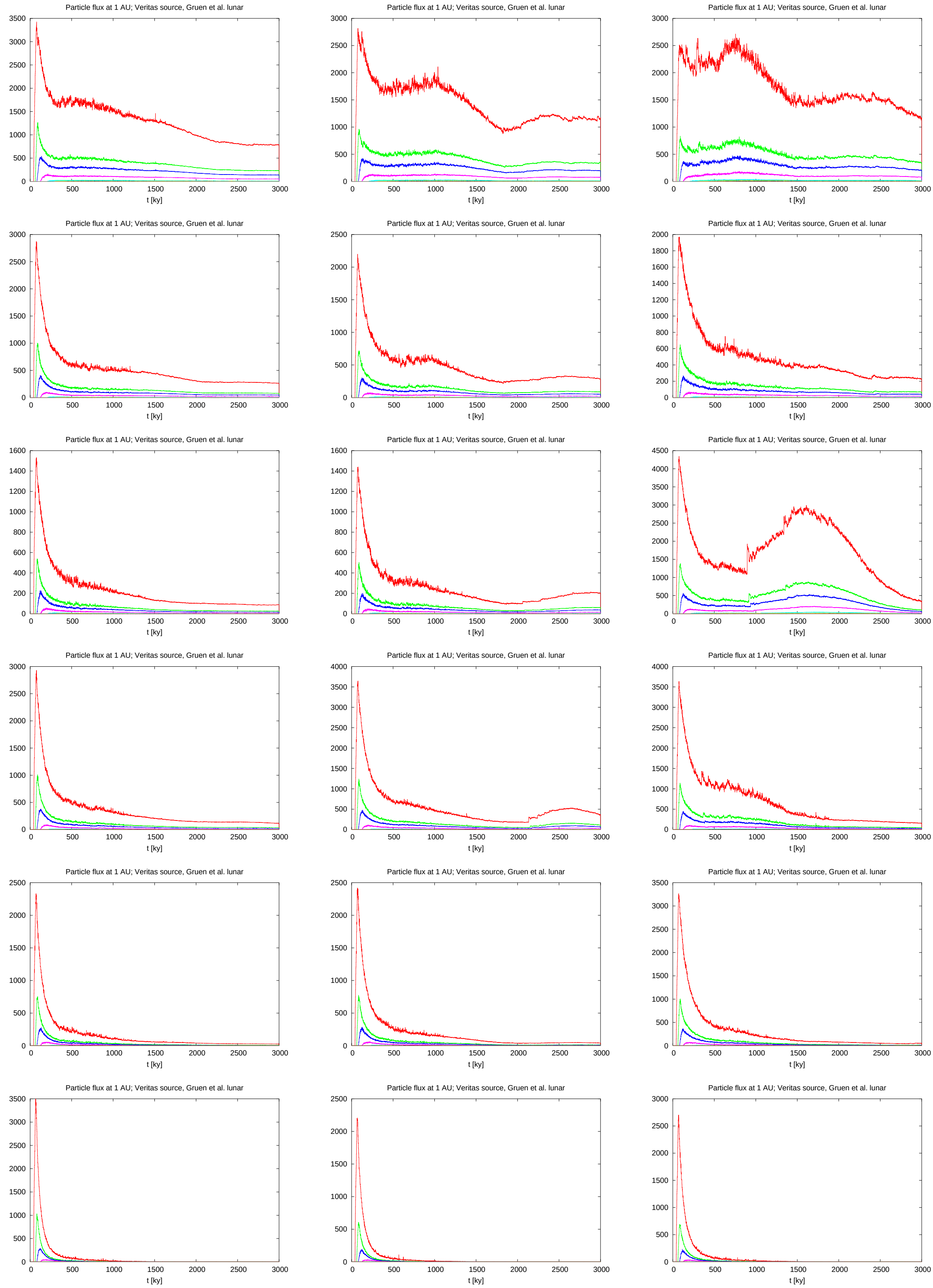

Figure 6: Models with a 'sliding knee': flux of the Veritas TPs through 1 AU heliocentric sphere as a function of time after the parent-body breakup. These panels correspond to $\tau_{\rm dec} = 0.5$ My. The three columns are for: (i) $\alpha_1 = -2$ (left), (ii) $\alpha_1 = -2.25$ (middle), and (iii) $\alpha_1 = -2.5$ (right). The six rows are for (from top to bottom): (i) $\alpha_2 = -3$, (ii) $\alpha_2 = -3.2$, (iii) $\alpha_2 = -3.25$, (iv) $\alpha_2 = -3.3$, (v) $\alpha_2 = -3.5$, and (vi) $\alpha_2 = -4$.

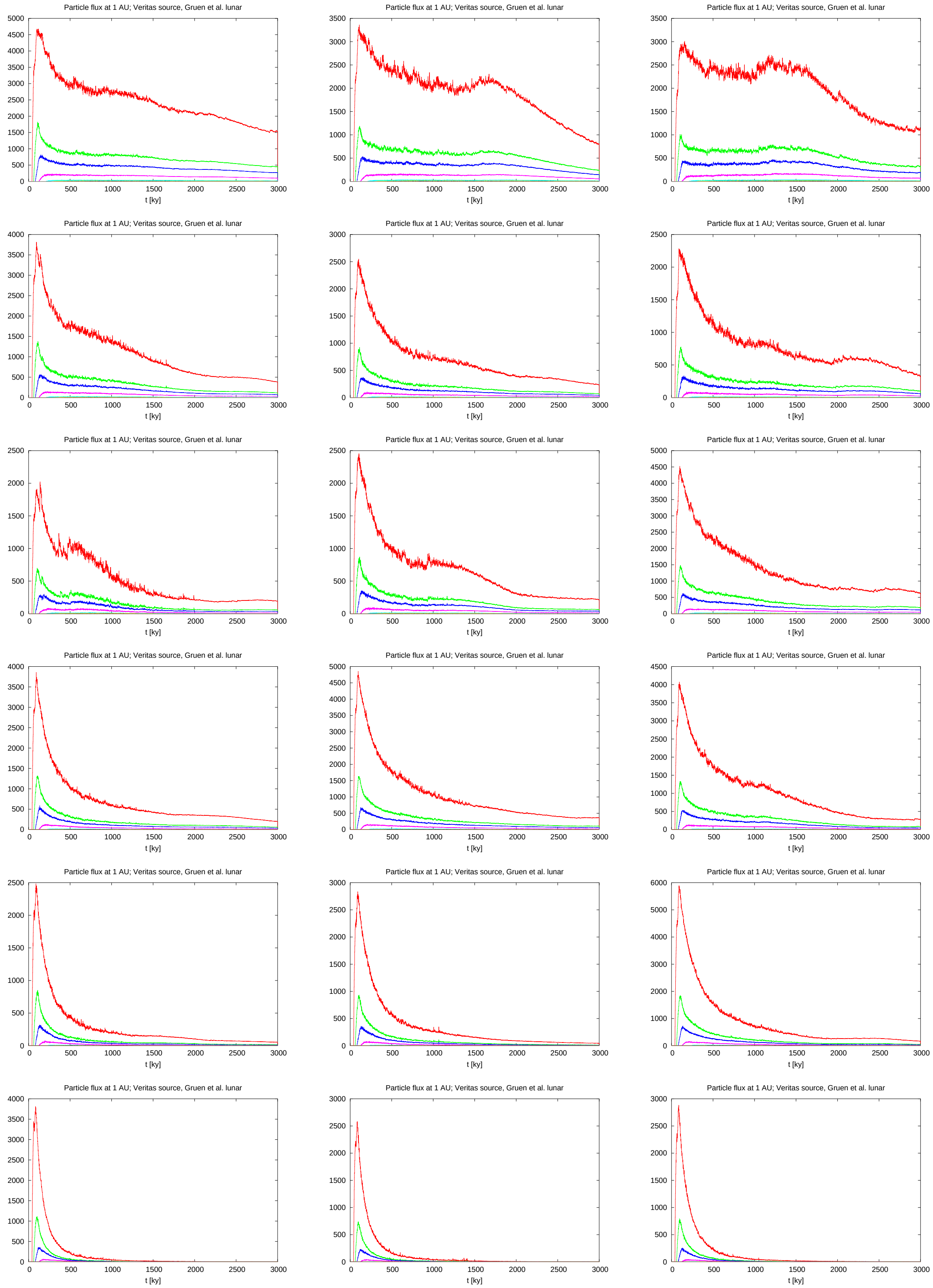

Figure 7: Models with a 'sliding knee': flux of the Veritas TPs through 1 AU heliocentric sphere as a function of time after the parent-body breakup. These panels correspond to $\tau_{\rm dec} = 1$ My. The three columns are for: (i) $\alpha_1 = -2$ (left), (ii) $\alpha_1 = -2.25$ (middle), and (iii) $\alpha_1 = -2.5$ (right). The six rows are for (from top to bottom): (i) $\alpha_2 = -3$, (ii) $\alpha_2 = -3.2$, (iii) $\alpha_2 = -3.25$, (iv) $\alpha_2 = -3.3$, (v) $\alpha_2 = -3.5$, and (vi) $\alpha_2 = -4$.

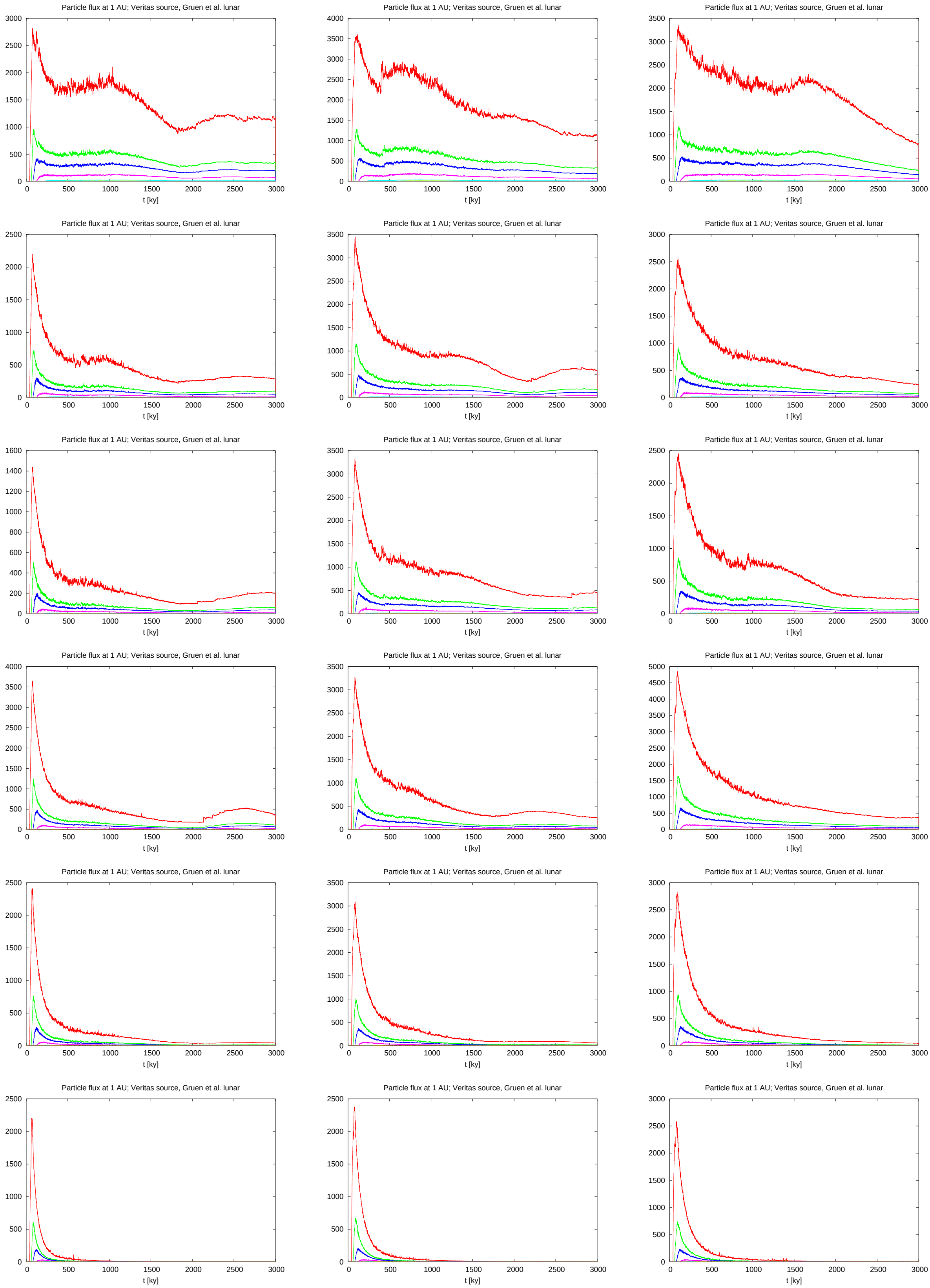

Figure 8: Models with a ‘sliding knee’: flux of the Veritas TPs through 1 AU heliocentric sphere as a function of time after the parent-body breakup. These panels correspond to $\alpha_1 = -2.25$. The three columns are for: (i) $\tau_{\rm dec} = 0.5$ My (left), (ii) $\tau_{\rm dec} = 0.75$ My (middle), and (iii) $\tau_{\rm dec} = 1$ My (right). The six rows are for (from top to bottom): (i) $\alpha_2 = -3$, (ii) $\alpha_2 = -3.2$, (iii) $\alpha_2 = -3.25$, (iv) $\alpha_2 = -3.3$, (v) $\alpha_2 = -3.5$, and (vi) $\alpha_2 = -4$.

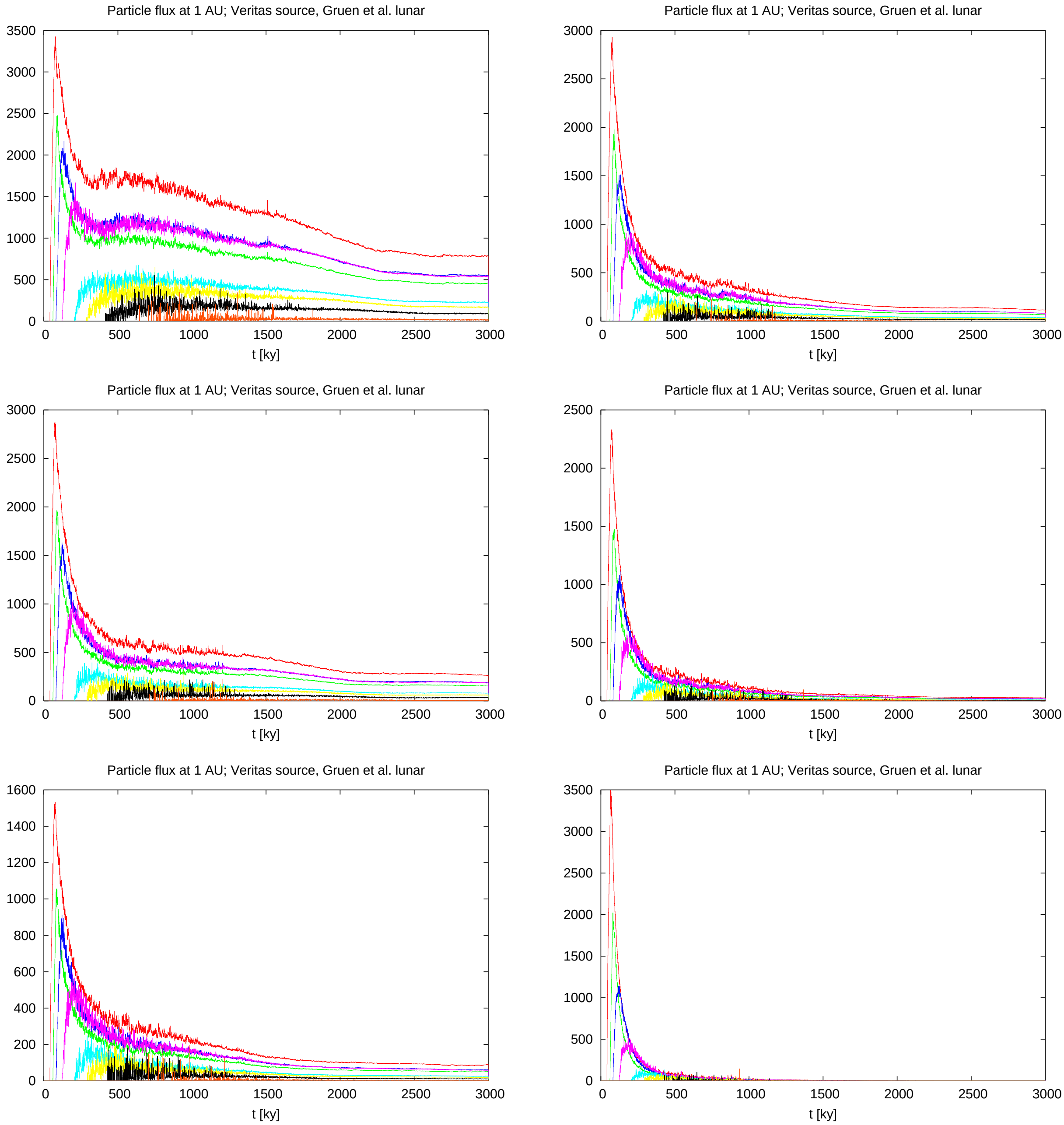

Figure 9: Models with a 'sliding knee': flux of the Veritas TPs through 1 AU heliocentric sphere as a function of time after the parent-body breakup. Here the number of particles (from Fig.2) is multiplied by scaling factor of their cross-section, thus increasing the sole of large particles wrt to small particles. Here $\alpha_1 = -2$ and $\tau_{\rm dec} = 0.5$ My fixed and different panels show results for different values of α_2: (i) -3 (left, top), (ii) -3.2 (left, middle), (iii) -3.25 (left, bottom), (iv) -3.3 (right, top), (v) -3.5 (right, middle), and (v) -4 (right, bottom). Different curves in each of the panels correspond to TPs in different size ranges. The uppermost red curve is for $(10-15)$ μm particles, green curve is for $(15-20)$ μm, blue curve is for $(20-30)$ μm, and so on.

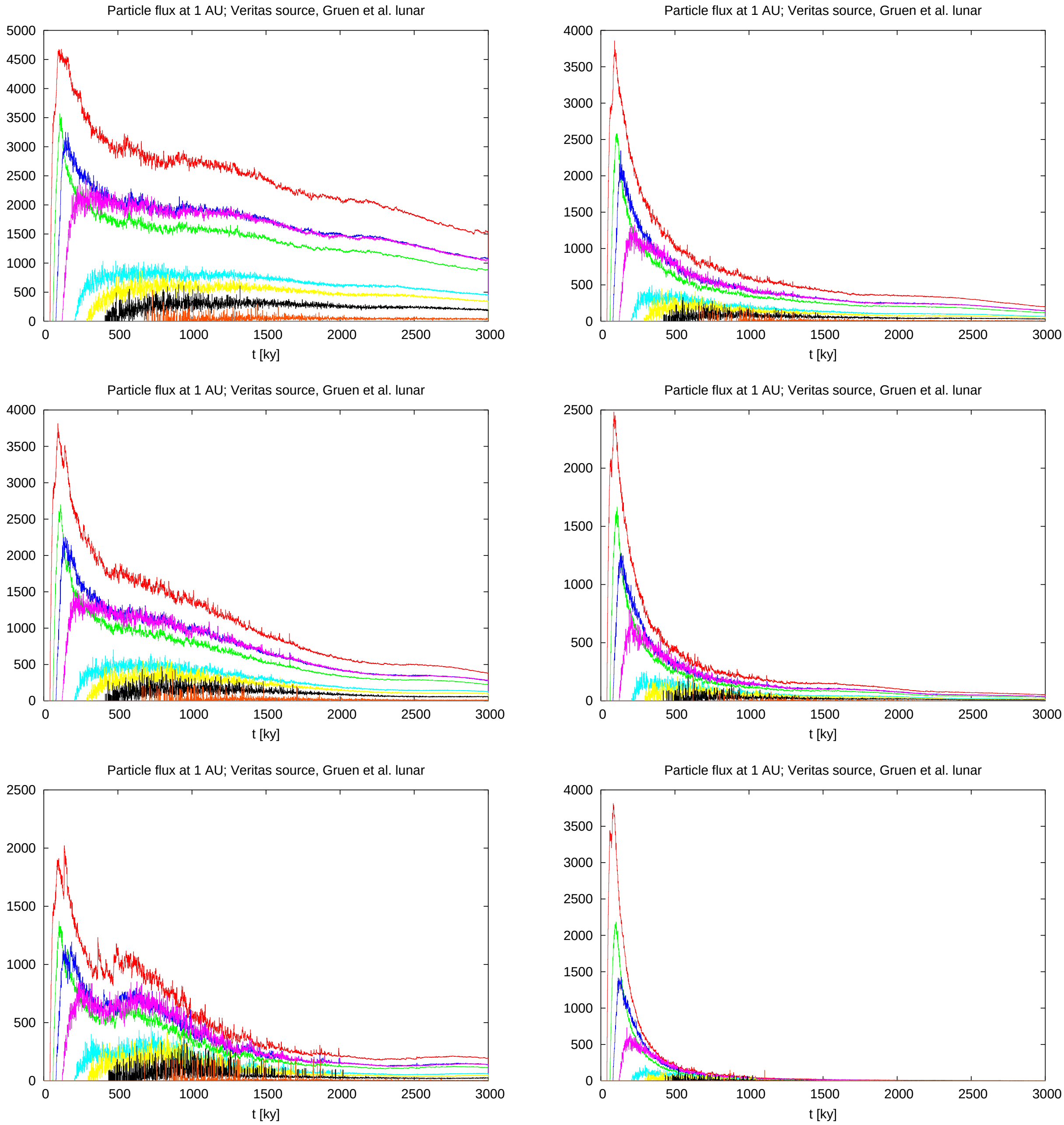

Figure 10: Models with a 'sliding knee': flux of the Veritas TPs through 1 AU heliocentric sphere as a function of time after the parent-body breakup. Here the number of particles (from Fig.3) is multiplied by scaling factor of their cross-section, thus increasing the sole of large particles wrt to small particles. Here $\alpha_1 = -2$ and $\tau_{\rm dec} = 1$ My fixed and different panels show results for different values of α_2: (i) -3 (left, top), (ii) -3.2 (left, middle), (iii) -3.25 (left, bottom), (iv) -3.3 (right, top), (v) -3.5 (right, middle), and (v) -4 (right, bottom). Different curves in each of the panels correspond to TPs in different size ranges. The uppermost red curve is for $(10 - 15)$ μm particles, green curve is for $(15 - 20)$ μm, blue curve is for $(20 - 30)$ μm, and so on.

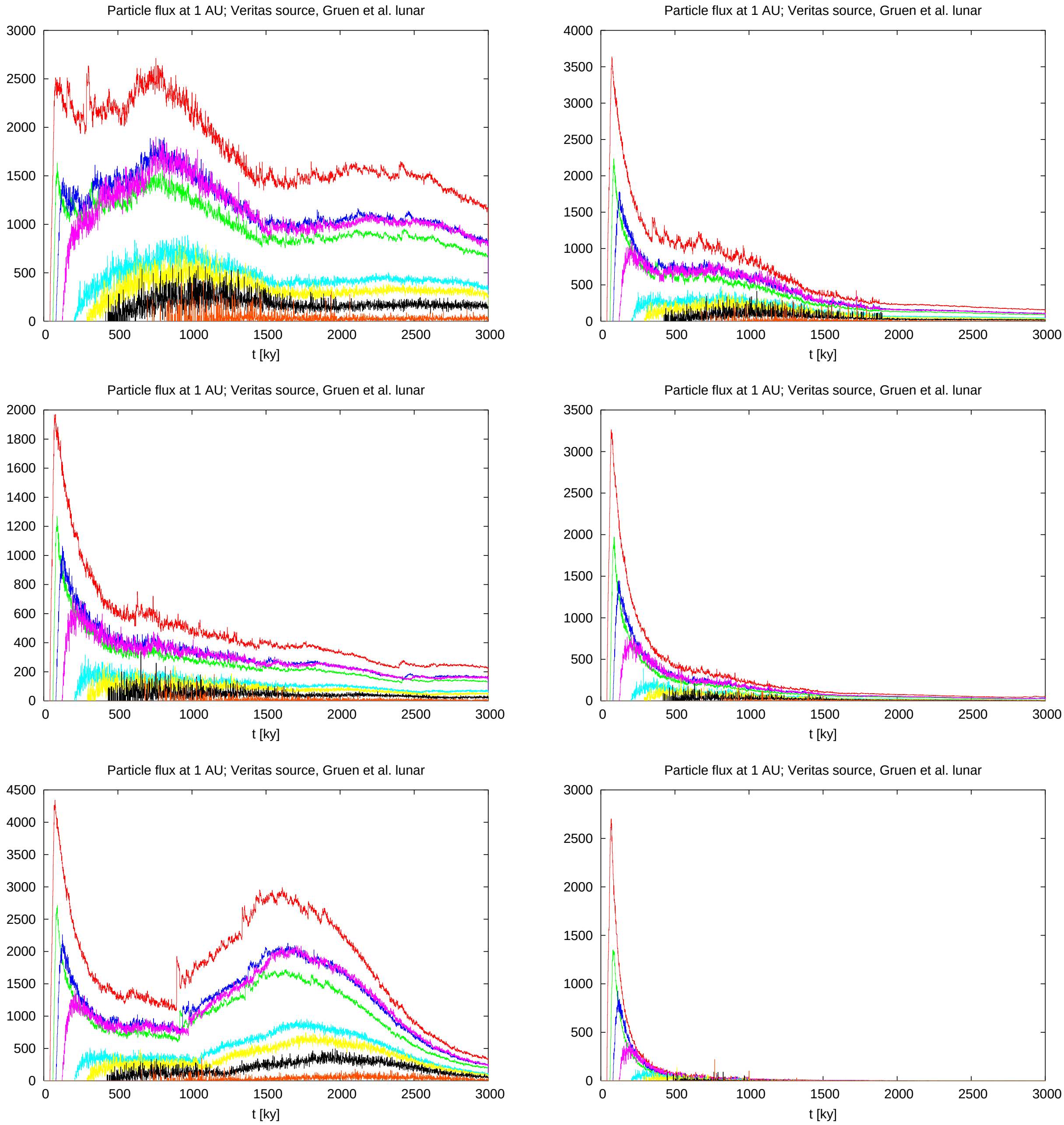

Figure 11: Models with a 'sliding knee': flux of the Veritas TPs through 1 AU heliocentric sphere as a function of time after the parent-body breakup. Here the number of particles (from Fig.4) is multiplied by scaling factor of their cross-section, thus increasing the sole of large particles wrt to small particles. Here $\alpha_1 = -2.5$ and $\tau_{\rm dec} = 0.5$ My fixed and different panels show results for different values of α_2: (i) -3 (left, top), (ii) -3.2 (left, middle), (iii) -3.25 (left, bottom), (iv) -3.3 (right, top), (v) -3.5 (right, middle), and (v) -4 (right, bottom). Different curves in each of the panels correspond to TPs in different size ranges. The uppermost red curve is for $(10-15)$ μm particles, green curve is for $(15-20)$ μm, blue curve is for $(20-30)$ μm, and so on.

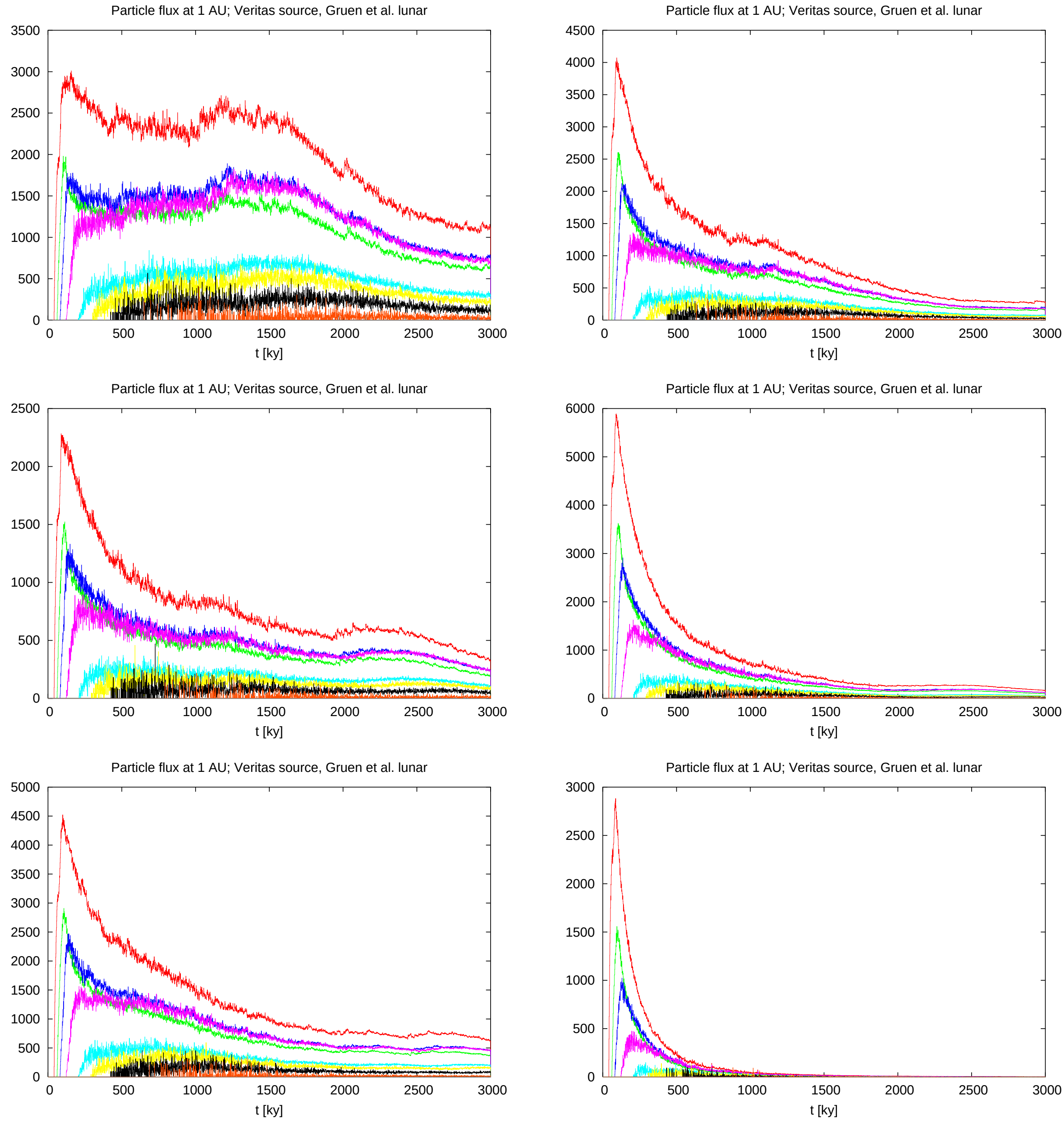

Figure 12: Models with a 'sliding knee': flux of the Veritas TPs through 1 AU heliocentric sphere as a function of time after the parent-body breakup. Here the number of particles (from Fig.5) is multiplied by scaling factor of their cross-section, thus increasing the sole of large particles wrt to small particles. Here $\alpha_1 = -2.5$ and $\tau_{\rm dec} = 1$ My fixed and different panels show results for different values of α_2: (i) -3 (left, top), (ii) -3.2 (left, middle), (iii) -3.25 (left, bottom), (iv) -3.3 (right, top), (v) -3.5 (right, middle), and (v) -4 (right, bottom). Different curves in each of the panels correspond to TPs in different size ranges. The uppermost red curve is for $(10-15)$ μm particles, green curve is for $(15-20)$ μm, blue curve is for $(20-30)$ μm, and so on.

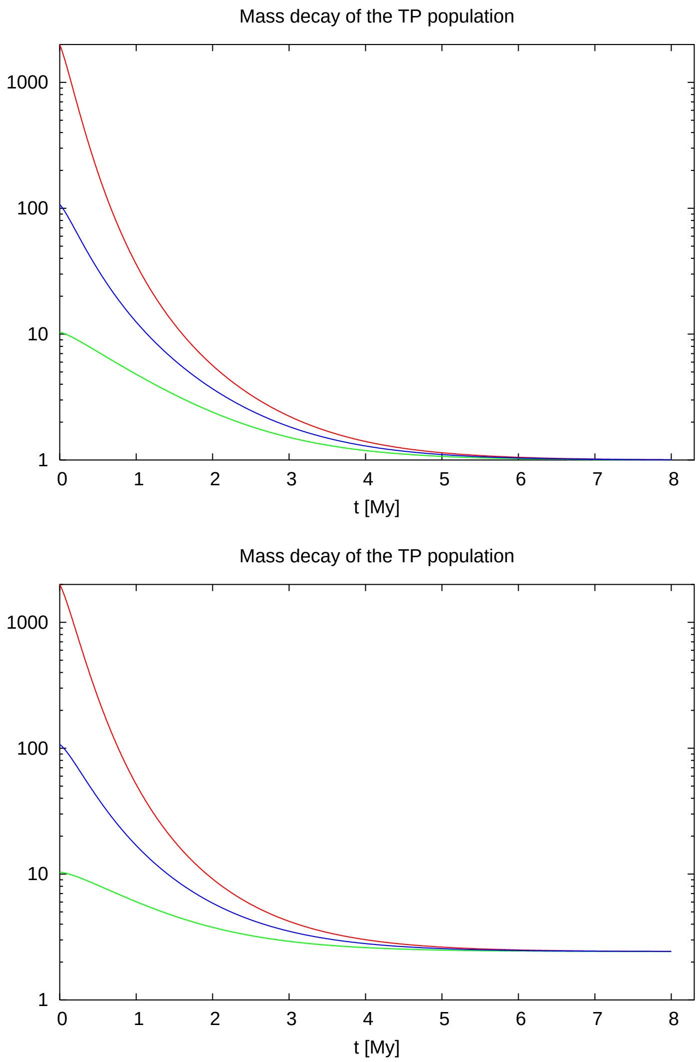

Figure 13: Models with a 'sliding knee'. Population mass decay as a function of time: (i) $\alpha_1 = -2$ (top) and (ii) $\alpha_1 = -2.5$ (bottom). The three curves are for $\alpha_2 = -4, -3.5$ and -3 from top to bottom. Here we fixed $\tau_{\rm dec} = 1$ My.

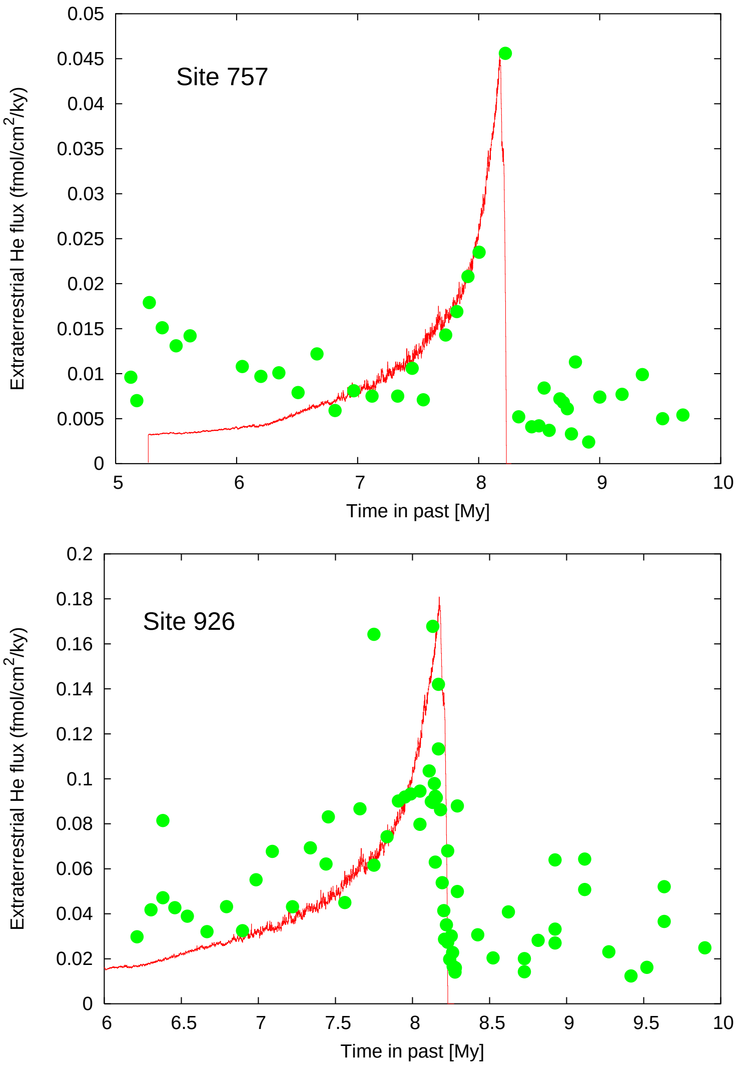

Figure 14: Comparison of model with $\alpha_1 = -2.25$, $\alpha_2 = -3.3$ and $\tau_{\rm dec} = 1$ My with data at Sites 757 and 926.

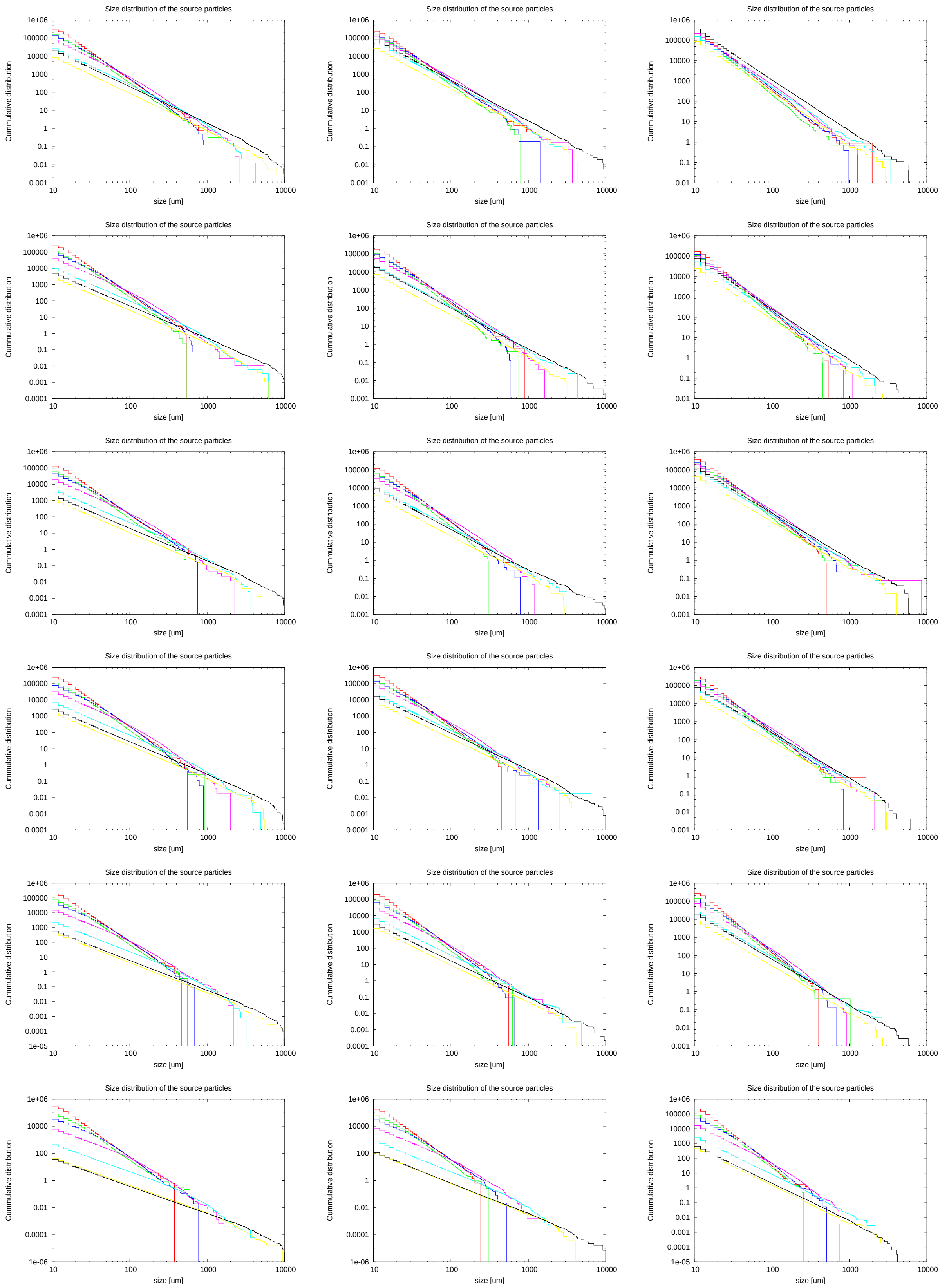

Figure 15: Models with a 'sliding knee': cummulative size distribution of TPs released in our simulation from the source (Veritas) in the time intervals $(0, 50)$ ky, $(50, 100)$ ky, $(100, 200)$ ky, $(200, 400)$ ky, $(400, 700)$ ky, $(700, 1000)$ ky and 1+ My. These panels correspond to $\tau_{\rm dec} = 0.5$ My. The three columns are for: (i) $\alpha_1 = -2$ (left), (ii) $\alpha_1 = -2.25$ (middle), and (iii) $\alpha_1 = -2.5$ (right). The six rows are for (from top to bottom): (i) $\alpha_2 = -3$, (ii) $\alpha_2 = -3.2$, (iii) $\alpha_2 = -3.25$, (iv) $\alpha_2 = -3.3$, (v) $\alpha_2 = -3.5$, and (vi) $\alpha_2 = -4$.

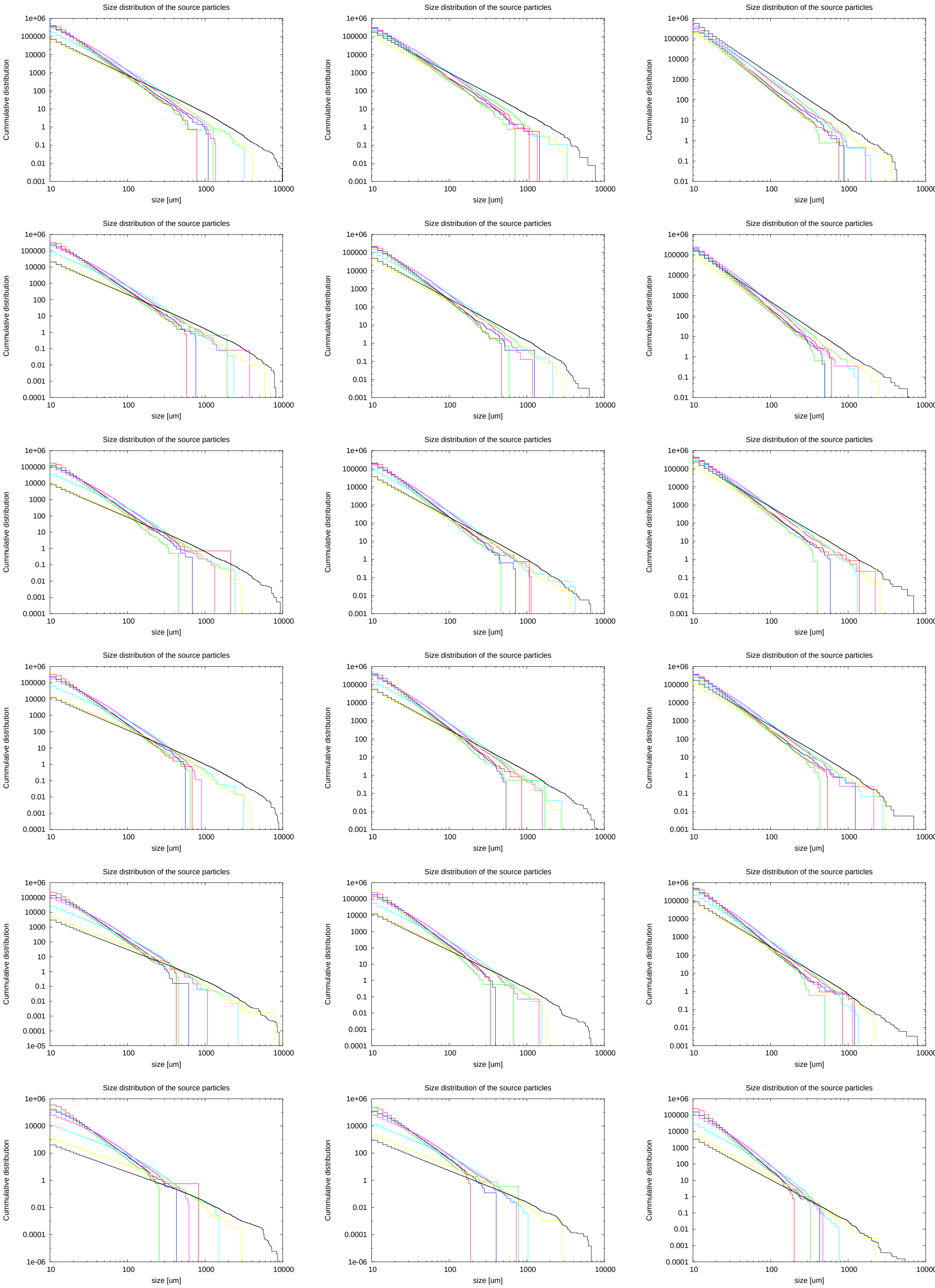

Figure 16: Models with a 'sliding knee': cummulative size distribution of TPs released in our simulation from the source (Veritas) in the time intervals $(0, 50)$ ky, $(50, 100)$ ky, $(100, 200)$ ky, $(200, 400)$ ky, $(400, 700)$ ky, $(700, 1000)$ ky and 1+ My. These panels correspond to $\tau_{\rm dec} = 1$ My. The three columns are for: (i) $\alpha_1 = -2$ (left), (ii) $\alpha_1 = -2.25$ (middle), and (iii) $\alpha_1 = -2.5$ (right). The six rows are for (from top to bottom): (i) $\alpha_2 = -3$, (ii) $\alpha_2 = -3.2$, (iii) $\alpha_2 = -3.25$, (iv) $\alpha_2 = -3.3$, (v) $\alpha_2 = -3.5$, and (vi) $\alpha_2 = -4$.

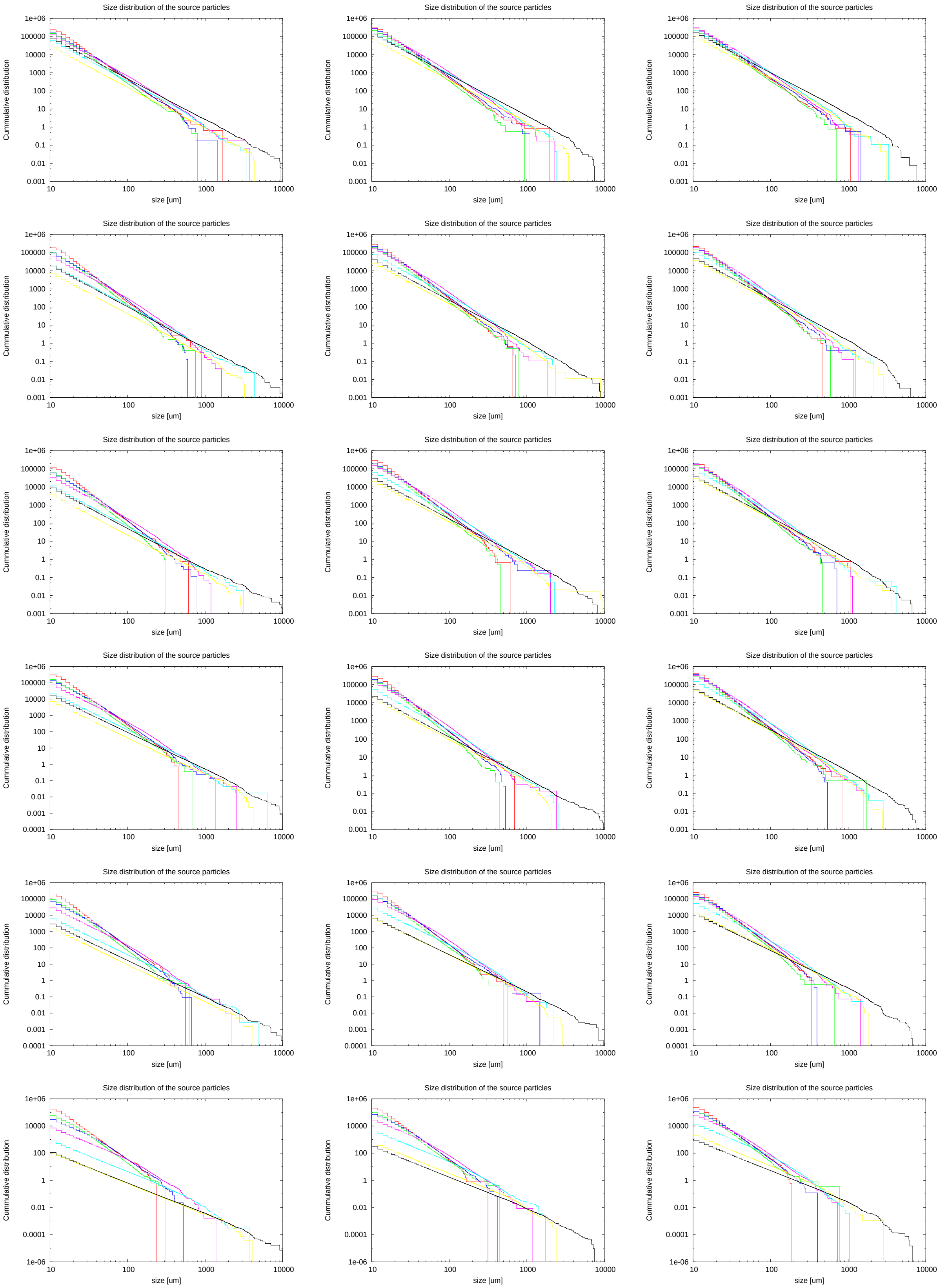

Figure 17: Models with a ‘sliding knee’: cummulative size distribution of TPs released in our simulation from the source (Veritas) in the time intervals $(0, 50)$ ky, $(50, 100)$ ky, $(100, 200)$ ky, $(200, 400)$ ky, $(400, 700)$ ky, $(700, 1000)$ ky and 1+ My. These panels correspond to $\alpha_1 = -2.25$. The three columns are for: (i) $\tau_{\rm dec} = 0.5$ My (left), (ii) $\tau_{\rm dec} = 0.75$ My (middle), and (iii) $\tau_{\rm dec} = 1$ My (right). The six rows are for (from top to bottom): (i) $\alpha_2 = -3$, (ii) $\alpha_2 = -3.2$, (iii) $\alpha_2 = -3.25$, (iv) $\alpha_2 = -3.3$, (v) $\alpha_2 = -3.5$, and (vi) $\alpha_2 = -4$.